European Journal of Pharmaceutics and Biopharmaceutics 70 (2008) 657–665

Contents lists available at ScienceDirect

European Journal of Pharmaceutics and Biopharmaceutics

journal homepage: www.elsevier.com/locate/ejpb

Research paper

Encapsulation of mitoxantrone into pegylated SUVs enhances its antineoplastic efficacy

ChunLei Li [a,*], JingXia Cui [b], CaiXia Wang [a], YinGui Li [a], HongWu Zhang [a], JinXu Wang [a], YanHui Li [a], Lan Zhang [a], Li Zhang [a], WenMin Guo [a], YongLi Wang [b]

[a] ZhongQi Pharmaceutical Technology (Shijiazhuang) Co., Ltd., Shijiazhuang City, PR China
[b] School of Pharmacy, Hebei Medical University, Shijiazhuang City, PR China

ARTICLE INFO

Article history:
Received 13 February 2008
Accepted in revised form 19 May 2008
Available online 6 June 2008

Keywords:
Mitoxantrone
Liposomes
Vesicle size
Drug release
Antitumor efficacy
Toxicity

ABSTRACT

Mitoxantrone (MIT) was encapsulated into 60, 80 and 100 nm pegylated hydrogenated soy phosphatidylcholine/cholesterol (HSPC/chol) vesicles using a transmembrane $(NH_4)_2SO_4$ gradient. In-vitro release studies revealed that small-sized formulation had fast drug-release rate. Acute toxicity studies performed in c57 mice proved that all pegylated liposomal MIT (plm) formulations could be well-tolerated at a dose of 9 mg/kg, significantly compared to severe toxicity induced by free mitoxantrone (f-M). In KM mice, plm60 was at least 2- to 3-fold less toxic than f-M. After intravenous injection, plm60 was slowly eliminated from plasma relative to f-M, resulting in about 6459-fold increase in AUC and its plasma kinetics exhibited dose dependence. In S-180 bearing KM mice, plm60 preferentially accumulated into tumor zone, with a ~12-fold increase in AUC and ~10-fold increase in C_{max} Furthermore, the accumulation of plm60 in almost all normal tissues markedly decreased. The antitumor efficacy of plm60 was also considerably enhanced. In L1210 ascitic tumor model, plm60 was the most efficacious which led to a ~70% long-term survival, significantly compared to 16–33% survival rate in plm80, plm100 and f-M groups at the same dose level (4 mg/kg). The antitumor efficacy of plm60 was more encouraging in L1210 liver metastasis model. At a dose of 6 mg/kg, ~90% animals receiving plm60 treatment could survive 60 days; however, in f-M group at the same dose, all the mice died at ~14 days post inoculation. Similarly, plm60 could effectively inhibit the growth of RM-1 tumor in BDF1 mice, resulting in marked increase in tumor doubling time at different dose levels relative to f-M. The improved antineoplastic effects could be ascribed to its small vesicle size, which allowed more drug release after the accumulation into tumor zone. Theoretical considerations revealed that the reduction of vesicle size could increase the specific area of MIT/sulfate precipitate inside the vesicle and the release constant K, which is inversely proportional to vesicle volume ($K = pA_m k_2 k_2' / ([H^+]_i^2 V_i)$).

1. Introduction

MIT is a synthetic antineoplastic anthracenedione that can inhibit the activity of topoisomerase II, interfere with RNA and cause the crosslink of DNA and strand breaks [1]. MIT has a cytocidal effect on both proliferating and non-proliferating cells, suggesting the lack of cell cycle phase specificity [2–3]. Similar to other anthracyclines, the main toxicity of MIT is cardiotoxicity [4–6]. Other toxicities such as primary neutropenia, bone marrow suppression and secondary acute myelogenous leukemia have also been reported in patients treated with MIT [7].

Encapsulation of MIT within liposomes might improve its therapeutic index because liposomes could preferentially accumulate into tumors due to enhanced permeability and retention effects [8]. MIT has two physiologically dissociated –NH– groups (Fig. 1), thus it could be loaded within liposomes via pH gradient or intercalated into lipid bilayers by the formation of complexes with negatively charged lipids [9–21]. The latter encapsulation method always leads to unstable formulations that cannot effectively retain MIT, especially in blood circulation. Following i.v. injection, MIT rapidly dissociates from lipid bilayers due to the dilution effect and the interaction with plasma components, thus exhibiting no clinical advantages [15–16]. Provided that active loading method such as pH gradient method is employed, the resulting LUV (large unilamellar vesicle) formulations usually have slow drug-release rate even after accumulation in local tumor and are less therapeutically effective than unentrapped MIT [18,20–21].

In the previous study, it was found that the release kinetics of doxorubicin from pegylated SUVs is much faster than that from LUVs, in which case, doxorubicin was encapsulated into liposomes via pH gradient method that relies on the transmembrane ammo-

* Corresponding author. ZhongQi Pharmaceutical Technology (Shijiazhuang) Co., Ltd., No. 276, ZhongShan West Road, Shijiazhuang City, Hebei Province 050051, PR China. Tel.: +86 0311 87891958; fax: +86 0311 87885233.
E-mail addresses: lcllib@hotmail.com, lcllib@yahoo.com (C. Li).

0939-6411/$ - see front matter © 2008 Elsevier B.V. All rights reserved.
doi:10.1016/j.ejpb.2008.05.019

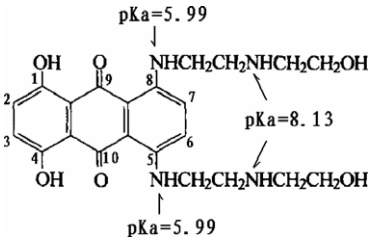

Fig. 1. The structure of mitoxantrone.

nium sulfate gradient [22]. Because MIT can also form precipitates with sulfate inside liposomes, we suspect that the reduction of vesicle size could also accelerate the release rate of MIT and lead to efficacious liposomal formulation. In this paper, we describe a novel liposomal MIT formulation, in which MIT was encapsulated in pegylated SUVs (with a size of ~60 nm) via ammonium sulfate gradient method. This formulation had accelerated drug-release rate and enhanced antineoplastic effects in RM-1, L1210 ascitic and liver metastasis tumor models.

2. Materials and methods

2.1. Materials

Mitoxantrone hydrochloride was provided by Chongqing Kailin Pharmaceutical Co., Ltd. (Chongqing, China). Hydrogenated soybean phosphatidylcholine (HSPC) was a kind gift from Degussa (Freising, Germany). *N*-(Carbonyl-methoxypolyethyleneglycol$_{2000}$)-1,2-distearoyl-sn-glycero-3-phosphoethanolamine, sodium salt (MPEG$_{2000}$-DSPE), was obtained from Genzyme Pharmaceuticals (Liestal, Switzerland). Cholesterol (chol) and Sephadex G-75 (medium) were obtained from the Sigma Chemical Company (St. Louis, MO). 1-Palmitoyl-2-stearoyl-sn-glycero-phosphocholine (PSPC), 1,2-stearoyl-sn-glycero-phosphocholine (DSPC), 1-palmitoyl-2-hydroxy-sn-glycero-3-phosphocholine (MPPC) and 1-stearoyl-2-hydroxy-sn-glycero-3-phosphocholine (MSPC) were purchased from Avanti Polar Lipids, Inc. (USA). Nucleopore polycarbonate filters (47-mm, 0.1- and 0.08-μm pore sizes) were obtained from Northernlipids, Inc. (Canada). All other chemicals used in this study were of analytical or high-performance liquid chromatography (HPLC) grade.

L1210 and RM-1 tumor cell lines were originally purchased from the Institute of Biochemistry and Cell Biology, Chinese Academy of Sciences (Shanghai, China). KM mice (8–10 weeks old) were obtained from Hebei Medical University. BDF1 and c57 mice were purchased from Vitalriver (Beijing, China).

2.2. Preparation of liposomes

Liposomes were prepared according to the following procedure. Briefly, the mixtures of HSPC, mPEG$_{2000}$-DSPE and chol (3:1:1, mass ratio) were solubilized in chloroform and dried to a thin lipid film under a stream of N_2 gas, followed by overnight incubation under vacuum to remove residual solvent. The dried lipid films were subsequently hydrated with 300 mM ammonium sulfate. The hydration process was performed at 60 °C for 1 h. The dispersion was extruded 8 times through polycarbonate filters of 0.10 μm (or 0.08 μm) at 60 °C employing a LiposoFast-100 jacketed extruder obtained from Avestin (Ottawa, Canada). This procedure formed unilamellar vesicles of 100 or 80 nm, and the resulting formulations were named plm100 and plm80. For the preparation of 60 nm vesicles, after hydration the dispersion was homogenized in M-110EH Microfluidizer® Processor (Microfluidics, USA) at 1500 bar. The resulting vesicles were ~60 nm in diameter and named plm60. The zeta average size of vesicles was analyzed using quasi-elastic light scattering (Zetasizer Nano ZS; Malvern Instruments, UK). Before analysis, the samples were diluted in 0.9% NaCl with a volume ratio of 1/200. The zeta potential of vesicles was also determined using Nano ZS, but the measurement was carried out in water after a 100-fold dilution. In both cases, DTS4.0 software was used to collect the data that were analyzed using "multinarrow modes".

2.3. Remote loading of liposomes

A transmembrane ammonium sulfate gradient was generated across the vesicles by exchanging the extraliposomal buffer using Sephadex G-75 columns. The buffer employed in the experiments was sucrose (300 mM)-histidine (10 mM) buffer (pH 7.5). Upon buffer exchange, empty liposomes with transmembrane ammonium sulfate gradient (total lipid concentration: 16 mg/mL) were mixed with 10 mg/mL MIT (10:1, v/v), resulting in a mass ratio of 1:16. The resulting mixture was incubated at 60 °C for 40 min to realize drug loading. After loading, the liposomal preparations were concentrated to a MIT concentration of 1 mg/mL using a Millipore Labscale TFF System (with 50,000 nominal molecular weight limit polysulfone filters).

For determining the loading efficiency, samples of the mixtures were taken and unentrapped MIT was removed by size-exclusion chromatography. Briefly, 100 μL samples were loaded onto Sephadex G-75 mini-column (56 mm × 8 mm i.d.) and then eluted using 0.9% NaCl solution.

2.4. Determination of lipid compositions and lyso PCs

A Waters HPLC system was used to determine lipid contents (HSPC, peg-lipid and cholesterol) and their degradation products, lyso PCs. The system was composed of 2690 liquid chromatograph and 410 RI detector and controlled by Millennium 32 software. For the measurement of lipid content, a zobax c18 (25 cm × 4.6 mm i.d., 5 μm particle size) was employed, which was maintained at 35 °C during the analysis. The mobile phase was a mixture of methanol, tetrahydrofuran (THF) and 0.17 mol/L ammonium acetate (94:5:1), running at a flow rate of 1 mL/min. The retention times for different components were 4.8 min (MPEG-DSPE), 8.6 min (cholesterol), and 10.1 min for the first peak of HSPC (PSPC) and 15.3 min for the second peak of HSPC (DSPC).

To detect the content of lyso PCs, the separation was carried out on a zobax NH_2 column (25 cm × 4.6 mm i.d., 5 μm particle size) at 30 °C at a flow rate of 1 mL/min. The mobile phase used consisted of acetonitrile, methanol and 8 mmol/L ammonium dihydrogenphosphate solution (pH 4.5, 69:26:5). Under these conditions, lysophospholipid standards (MSPC and MPPC) were consistently eluted as two peaks, which corresponded to two positional isomers of lysophospholipids. Since HSPC consisted of both PSPC and DSPC, its degradation products contained MSPC and MPPC, and their positional isomers. Using this method, these four lyso PCs could be effectively separated with retention times ranging from 9.5 to 15.6 min.

In both cases, 2 mL of samples was diluted to 10 mL using chloroform–methanol (1:2) mixture and then the resulting solutions were injected into HPLC with injection volume of 10 μL for the analysis of lipid compositions and 100 μL for the detection of lyso PCs.

2.5. In-vitro release studies

Method I. Liposomal MIT formulations, at a concentration of 0.46 mM HSPC, were diluted in release buffer I (50% isotonic glu-

cose solution buffered with 10 mM histidine to pH 7.5 and 50% human plasma). Then 2 mL of diluted liposomes was placed in the dialysis tubing with a molecular weight cutoff of 10 kDa and dialyzed against 50 mL of release buffer I containing penicillin and streptomycin (100 μg/mL for each antibiotic).

Method II. Liposome-entrapped MIT was diluted to similar HSPC concentration with release buffer II, which had the same composition as buffer I except that buffer II contained 20 mM NH_4Cl. Then 2 mL of diluted liposomes was placed in the dialysis tubing and dialyzed against 50 mL release buffer II supplemented with two antibiotics.

The dialysis process was performed at 37 °C. At various time points, aliquots were withdrawn and stored at −20 °C until analysis. The samples were treated and analyzed using the method mentioned in PK studies.

2.6. Acute toxicity evaluation

The maximum tolerated dose of different plm formulations following i.v. administration was first sought in healthy male c57 mice. Briefly, the drug was administrated via tail vein in groups of two mice, beginning with the dose of 10 mg/kg MIT and continuing with the dose escalation factor of 1.19 until a dose level of 20 mg/kg was achieved (dose levels: 10.0, 11.9, 14.2, 16.9 and 20.0 mg/kg). If during the observation period, there was no mortality, irreversible morbidity, or severe body weight loss (consistent loss in excess of 20% of original weight maintained for 72 h), the highest administrated dose was considered as the acute single injection maximum tolerated dose. Based on the results from the dose-seeking step, plm formulations and f-M were administrated to male c57 mice at a dose of 9 mg/kg ($n = 5$). The inclusion of f-M group was just for the purpose of comparison.

To further test plm60 and f-M mediated acute toxicity, tumor-free KM mice were employed. Plm60 and f-M were injected into mice at a dose of 7.2, 12 and 20 mg/kg (5/sex/group).

In all cases, qualified animal-care technicians monitored the mice for weight loss and other signs of stress/toxicity for a period of 21 days. Because death cannot be used as an end point, mice were sacrificed at the first sign of distress for humane consideration. After 21 days, all remaining animals were terminated and necropsies were conducted to identify any additional drug toxicities. The difference in body weights was examined by a series of Independent Samples T-test and $p < 0.05$ was considered to be statistically significant.

2.7. Pharmacokinetic and biodistribution studies

Plasma pharmacokinetic analysis was performed in normal KM mice and KM mice bearing a s.c. S-180 tumor (0.5–0.6 cm^3) were used in tissue distribution studies.

For PK studies, KM mice received injections of 1, 2 and 4 mg/kg single i.v. bolus dose of plm60 and 2 mg/kg f-M via tail vein. Blood samples were obtained via cardiac puncture under anesthesia and collected in Eppendorf tubes containing sodium heparin as an anticoagulant. For tumor-bearing mice, plm60 and f-M were administrated at a dose of 4 mg/kg. At the indicated time points, mice were euthanized. Liver, spleen, kidney, lung, heart, intestine and tumor were rapidly excised, rinsed in ice-cold normal saline and snap-frozen. Blood samples were centrifuged at 2500 rpm for 10 min to separate the plasma. The plasma and tissue samples were stored at −20 °C until additional analysis.

MIT concentrations in plasma and in normal and tumor tissue samples were determined using HPLC method. Before analysis, mouse tissues were firstly homogenized using a tissue tearor equipped with a 7-mm probe (Biospec Products, Inc., USA). A 10% (w/v) homogenate was prepared in 20% ascorbic acid solutions. For 150-μL plasma or tissue homogenate, 150-μL extraction solution (methanol containing 0.5 M HCl: acetonitrile (90/10, v/v)) was added. The resulting mixture was vortexed and permitted to precipitate at −20 °C for at least 1 h and then centrifuged at 20,000*g* for 10 min. The supernatant was collected for analysis. The injection volume for samples was 20 μL.

A Waters HPLC system controlled by Millennium 32 software was used for chromatographic analysis, which was composed of 2690 liquid chromatograph and 996 diode array detector. The HPLC separations were achieved using a Zorbax C18, 150 mm × 4 mm i.d., 5 μm particle-size column. The isocratic mobile phase was a mixture of acetonitrile and a solution containing 6.0 g/L of sodium 1-heptanesulfonate and 9.0 mL/L of glacial acetic acid (30:70, v/v), running at a flow rate of 1 mL/min. Detection was accomplished at 650 nm. MIT was eluted at ∼10 min. The recovery of drug was >95% and the standard curve with an *r*-value of 0.999.

The pharmacokinetic variables, tissue AUC, C_{max} were calculated using DAS 2.0 software (the net for drug evaluation of China).

2.8. Antitumor efficacy study

Male BDF1 mice were inoculated i.p. with 5×10^5 (or i.v. with 5×10^4) L1210 murine tumor cells, derived from the ascitic fluid of a previously infected BDF1 mouse. Free MIT or liposome-encapsulated MITs were administrated via a lateral tail vein, 24 h after tumor cell inoculation. Animal weights were monitored daily and mortality was determined up to 60 days. Because death cannot be used as an end point, mice were sacrificed at the first sign of distress. The data were analyzed with SPSS 11.5 version software (survival analysis).

RM-1 prostate tumor cells were injected s.c. (5×10^5 cells/mouse) in the right flank region of BDF1 mice. Tumors were allowed to grow to a mean tumor volume of 0.2 cm^3 before initiation of treatment. Tumor-bearing mice were randomly divided into 5 groups ($n = 11$). The treatment groups were given a single i.v. injection of plm60 and f-M (4 and 6 mg MIT/kg), respectively. Control mice were treated with an isotonic sucrose–histidine solution. The tumor volume (V) was calculated according to the equation $(\pi/6) \times \text{width}^2 \times \text{length}$. Animal weight and tumor sizes were monitored every 2 (or 3) days. For statistical analysis, the tumor volumes of treatment group and control mice at each time point were examined using one-way analysis of variance. Post-hoc comparison of the means of individual groups was performed using LSD test. In all cases, $p < 0.05$ was considered to be statistically significant.

3. Results

3.1. The characterization of plm formulations

MIT was loaded into pegylated liposomes exhibiting a transmembrane ammonium sulfate gradient. Prior to loading, empty vesicles with entrapped ammonium sulfate were exchanged into a pH 7.5 sucrose/histidine buffer. For all the formulations, the% encapsulation value was ∼100% and the drug/lipid mass ratio was 1:16. Despite the vesicles having been prepared using a different size-reduction technology (extrusion or microfluidization), all the formulations had a narrow size distribution, with a polydispersion index ranging from 0.05 to 0.09 (Table 1). Zeta potential measurement showed that the difference in the vesicle size might exert an influence on the charges carried by the vesicles. Although these formulations had the same bilayer composition, small vesicles were more negatively charged than the large vesicles, indicating that more peg-lipids redistributed in the outer layer during the preparation procedure (under physiological pH values, HSPC is neutral, but peg-DSPE is negatively charged).

Table 1
The characterization of plm formulations

Formulations	Size (nm)	PDI	Zeta potential (−mV)	Loading efficiency (%)	Lyso PC (mg/mL)	HSPC (mg/mL)	Peg-lipid (mg/mL)	Chol (mg/mL)
Plm60	62.27 ± 0.34	0.092 ± 0.005	−42.58 ± 1.70	99.00	0.06	9.58	3.14	3.22
Plm80	85.17 ± 0.23	0.066 ± 0.007	−36.30 ± 1.65	99.01	0.07	9.49	3.08	3.18
Plm100	102.38 ± 0.68	0.047 ± 0.024	−33.41 ± 1.43	99.33	0.06	9.64	3.29	3.24

For the determination of vesicle size and zeta potential, the samples were diluted with 0.9% NaCl or water for injection, respectively. The measurement was performed at 25 °C using Zetasizer Nano ZS (Malvern Instruments, UK). DTS software (version 4.0) was employed to collect the data that were analyzed using "multinarrow modes". The loading efficiency was determined using size-exclusion chromatography. To assay the lipid content and lyso PC, two HPLC methods based on refractive index detector were employed. In all the cases, the data are presented as means from at least three repeated experiments. All the RSD (relative standard deviations) for loading efficiency, lipid composition and lyso PC were <2% and not given. PDI, polydispersion index.

For all the formulations, the HSPC, chol, and peg-DSPE contents were very close to the theoretical values (9.60, 3.20 and 3.20 mg/mL) and lyso PC was only 0.06–0.07 mg/mL, accounting for ~0.9% HSPC hydrolysis. It was not surprising that the use of Microfluidizer did not induce the increase of lyso PC in plm60, because the homogenization time was short and the interactive and auxiliary chambers had been cooled during the homogenization process (not larger than 65 °C).

3.2. In-vitro release

Drug-release experiments were first performed in ammonium chloride/histidine/glucose medium (isotonic, pH 7.5) using dialysis method. For all formulations, no obvious drug release was observed even when the NH_4Cl concentration was elevated to 40 mM. In contrast, under the same release conditions, ammonium could effectively trigger the release of doxorubicin from small pegylated vesicles with the same formulation composition [22]. To compare the release kinetics of different formulations, 50% plasma was employed as release medium. Overall the experiment period, plm80 and plm100 still could not release MIT, but plm60 exhibited a release $t_{1/2}$ value of 56.4 h. If the 50% plasma was supplemented with 20 mM NH_4Cl, the release $t_{1/2}$ values of MIT from plm80 and plm60 were 36.7 and 26.2 h, respectively. These results clearly revealed the difference in the release kinetics, indicating that small-sized formulations had fast drug-release rates (Fig. 2).

3.3. Acute toxicity

Dose-seeking studies using a small number of mice revealed that decreased vesicle size resulted in increased acute toxicity. The highest dose levels at which we could not observe mortality, irreversible morbidity, or severe body weight loss were 16.9 (plm100), 14.2 (plm80) and 14.2 (plm60) mg/kg. Using this method, the obtained maximum tolerated doses for plm80 and plm60 were roughly equivalent, but plm60 was still a little more toxic than plm80, comparing body weight versus time curves. All plm formulations, when administrated at a dose of $\geqslant$12 mg/kg, induced visible accumulation of MIT into paws of animals. The paws of animals became blue in a dose-dependent manner (MIT has a blue black color). The degree of MIT deposited into paws was as follows: pm100 > plm80 > plm60.

Since the accumulation of pegylated liposomes (especially when they encapsulated cytotoxic drugs) into skin might induce foot–hand syndromes, which are the dose-limiting toxicities of Doxil/Caelyx in the clinical practice [8], the toxicities of plm formulations and free MIT were compared at a reduced dose level (9 mg/kg) in c57 mice. At this dose level, the accumulation of MIT into skin was not evident besides plm100 group. All plm formulations exerted no effects on body weight for 21 days. But for f-M, a ~30% body weight loss was observed at 10 days post injection in one mice. Furthermore, three mice were sacrificed at days 7, 8 and 9 for humane consideration.

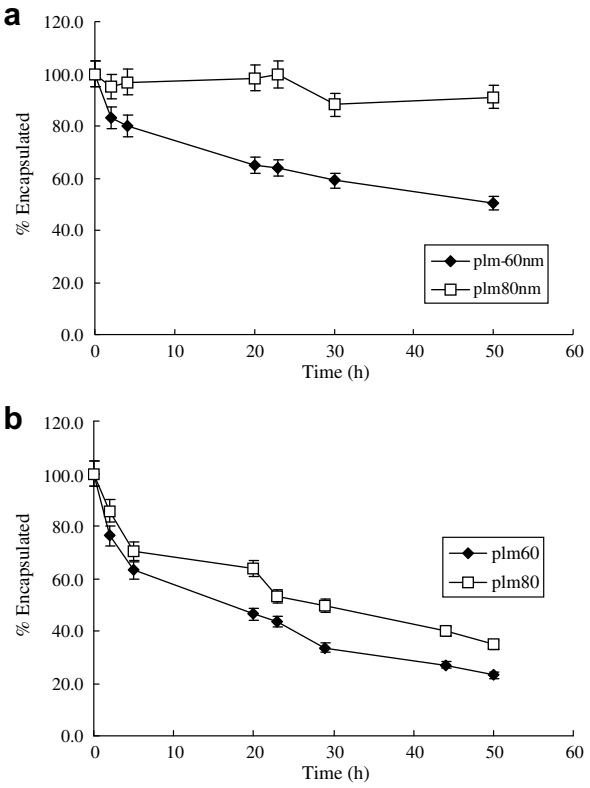

Fig. 2. In-vitro release of plm formulations with different vesicle sizes. The release experiments were performed in (a) 50% human plasma and 50% isotonic glucose solution buffered with 10 mM histidine to pH 7.5 (GHS) and (b) 50% plasma and 50% GHS supplemented with 20 mM NH_4Cl. In both cases, the plm formulation was diluted to a HSPC concentration of 0.46 mM and 2 mL sample was dialyzed against 50 mM release medium at 37 °C. Data points represent the mean values calculated from three samples.

Subsequent experiments further proved the low toxicity of plm60 compared to f-M. Plm60 and f-M were administrated to KM mice at a dose ranging from 7.2 mg to 20 mg/kg. At high dose levels (20 and 12 mg/kg), median survival time of plm60 group was significantly longer than that of f-M group ($p < 0.05$) (Table 2). When the animals received i.v. injection of plm60 and f-M at a dose of 7.2 mg/kg, all the animals could survive 21 days. In plm60 group the body weight continuously increased, but a ~23% (and 9%) body weight loss occurred in female (and male) mice receiving f-M injection.

Based on our observation, the toxicities of free MIT in mice included significant white blood-cell decrease, gastrointestinal mucosa necrosis, and acute hepatic injury revealed by increased ALT

Table 2
Acute toxicity of plm60 and f-M in KM mice

Treatment group	Dose (mg/kg)	No. of survivors (day 21)	Mean survival time[a]	Median survival time[a]
f-M	20	0/10	8.30 ± 1.36	7.00 ± 0.29
f-M	12	2/10	13.70 ± 1.44	12.00 ± 0.52
f-M	7.2	10/10	n.a.	n.a.
Plm60	20	8/10	19.50 ± 1.01	n.a.
Plm60	12	10/10	n.a.	n.a.
Plm60	7.2	10/10	n.a.	n.a.

Plm60 and f-M were injected into KM mice via tail vein at doses of 7.2, 12 and 20 mg/kg. The mice were monitored for a period of 21 days by qualified animal-care technicians. Because death cannot be used as end point, mice were evaluated twice daily and sacrificed at the first sign of distress.

[a] To calculate mean and median survival times, survivors after 21 days were assigned survival times of 21 days. n.a., not applicable.

and AST, toxic effects on hematopoietic and lymphoid tissues of spleen and bone marrow. At the same dose, the toxicities of plm were much lower than those of free MIT. For plm groups, the main toxicities were gastrointestinal mucosa necrosis, acute hepatic injury and skin toxicity. However, even at high dose, we did not observe the signs of heart toxicity in free MIT and plm groups, probably because of the low cumulative doses and relatively brief duration of each study.

3.4. Plasma pharmacokinetics and biodistribution

Since plm60 had reduced toxicity, the least skin toxicity and a fast drug-release rate, it was selected to perform PK and BD studies. As shown in Fig. 3, the encapsulation of MIT into pegylated small vesicles markedly altered the PK of MIT. In comparison with f-M, the AUC value of plm60 at the same dose level (2 mg/kg) was 775.1 μg h/mL, accounting for 6459-folds higher than that of f-M.

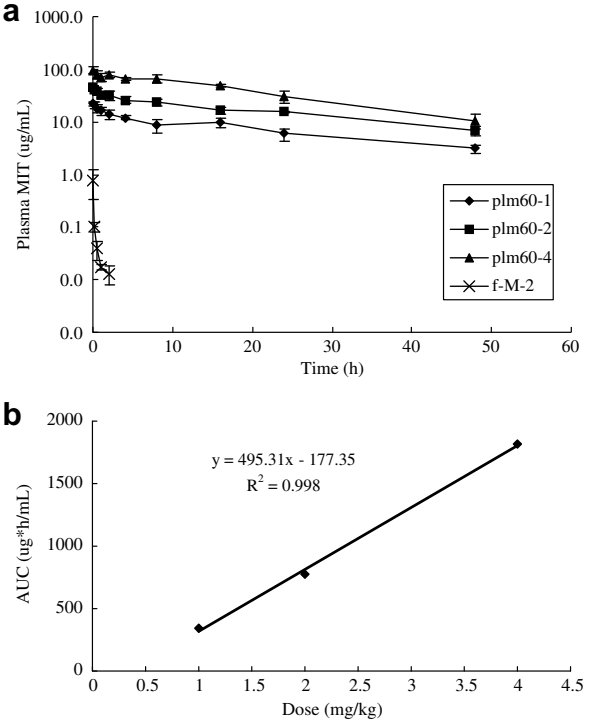

Fig. 3. (a) Plasma pharmacokinetics of plm60 and f-M in normal KM mice. Plm60 was administrated to KM mice at 1, 2 and 4 mg/kg and f-M at 2 mg/kg via tail vein ($n = 5$). (b) Dose dependence of plm60. The plasma AUC following i.v. administration of plm60 was plotted versus dose level.

Correspondingly, the half-life of plm60 was also considerably increased, with a $t_{1/2}$ of 16.2–19.0 h. In contrast, f-M was rapidly cleared from circulation with a $t_{1/2}$ value smaller than 5 min. Another phenomenon that should be noted was that plm60 exhibited linear kinetics and the regression equation of AUC versus dose had an r-value of 0.999. The PK of plm60 was similar to that of pld (pegylated liposomal doxorubicin), both with prolonged $t_{1/2}$ and increased AUC, which is the characteristic of pegylated liposomes provided that the drug could be effectively retained by vesicles in circulation [22–23]. Previous studies have proved that in blood, ~96% doxorubicin was in the form of liposomal encapsulation [24]. Taking into account the fact that in in-vitro release study, plm60 was hard to release drug relative to pld, one might suggest that the leakage of MIT from plm60 was negligible.

Tissue level of MIT was determined in S-180 bearing mice. Compared to f-M, plm60 preferentially accumulated into tumor zones, instead of normal tissues (Table 3). Tumor AUC in plm60-treated animals was ~12-folds higher than in mice treated with the same dose of f-M. Peak MIT concentration in tumor was higher and occurred later than after f-M treatment.

Except in liver, the C_{max} in all normal tissues following injection of plm60 significantly decreased. The C_{max} in heart, a primary target organ for MIT-associated toxicity, was 26% lower in plm60 group than in f-M group. Because cardiotoxicity is related to C_{max} but not to AUC, this result might imply the reduced cardiotoxicity of plm60 [4–6]. Furthermore, the assay in this study could not distinguish between liposome-entrapped (non-bioavailable) and free MIT (bioavailable), and the increased AUC and C_{max} in liver following plm60 administration might not mean the increased liver toxicity of plm60. Acute toxicity study also supported the low toxicity of plm60.

3.5. Antineoplastic activity

Based on the above experiments, liposome formulations with different sizes exhibited different drug-release kinetics. To explore the size effects on antineoplastic activity, L1210 ascitic tumor model was employed. As revealed by Table 4, all formulations could markedly prolong the survival time (mean and median) of tumor-bearing mice, relative to control group. It is interesting to note that the survival time of mice increased when the animal was treated with small-sized vesicles. This phenomenon might be ascribed to the fast drug-release rate of small-sized formulations. Previous studies have pointed out that MIT was hard to be released from 100 nm DSPC vesicles and the resulting liposomal formulation exhibited no therapeutic advantages in comparison with f-M [18,20–21]. Fast-release formulations might overcome this difficulty because more drugs would become available in tumor zone after the accumulation of vesicles. The results also revealed that plm60 was more efficacious than f-M at 4 mg/kg and that the activity of f-M was equivalent to that of plm80.

The antineoplastic effect of plm60 was examined in L1210 liver metastasis model, too. The data are presented in Table 5. The i.v. inoculation of L1210 cells resulted in rapid death in control group with a mean (or median) survival time of ~11 days. The administration of plm60 (or f-M) could significantly prolong the survival time of mice relative to the control group, and the antitumor effects were dose-dependent. As observed in other tumor models, plm60 showed superior activity to the f-M. The antitumor effect of 2 mg/kg plm60 was a little stronger than that of 6 mg/kg f-M. When plm60 was administrated at a dose of 8 mg/kg, all the treated mice survived 60 days.

The growth rate of RM-1 tumor in BDF1 mice was slow compared to other allograft tumor models (e.g. S-180 in KM mice). The tumor reached to a volume of ~200 mm^3 two weeks after inoculation, and then plm60 and f-M were administrated to animals at a dose of 4 (or 6) mg MIT/kg. Regression analysis revealed

Table 3
Comparison of tissue and tumor pharmacokinetics of plm60 and f-M

Tissues	Plm60 AUC_{Mit} (μg/g h) (1–24 h)	f-M AUC_{Mit} (μg/g h) (1–24 h)	Ratio of AUC[a]	Plm60 *C* range (μg/g)	f-M *C* range (μg/g)	% Change in C_{max}[b]
Heart	69.64	75.90	0.92	4.01–2.06	5.39–2.94	−25.60
Liver***	136.84	61.69	2.22	6.78–4.52	4.77–1.94	42.14
Spleen	135.05	121.43	1.11	7.56–4.36	7.75–3.77	−2.45
Lung**	119.19	178.23	0.67	8.44–2.89	10.21–7.02	−17.34
Kidney***	155.08	281.33	0.55	7.12–5.82	18.24–7.46	−60.96
Intestine*	53.05	66.79	0.79	2.42–1.66	3.94–1.53	−38.58
Tumor***	247.04	19.43	12.71	14.75–2.96	1.26–0.63	1070.63

Tissue and tumor levels of MIT were determined in S-180 bearing KM mice following i.v. administration of 4 mg/kg plm60 and f-M. All variables were calculated using DAS2.0 software.
[a] $AUC_{plm60}/AUC_{f\text{-}M}$.
[b] $C_{plm60} - C_{f\text{-}M}/C_{f\text{-}M}$.
* $p < 0.05$.
** $p < 0.01$.
*** $p < 0.001$.

Table 4
Antitumor efficacy of liposome-entrapped MIT formulations with different vesicle sizes in L1210 ascitic tumor model

Treatment group	Dose (mg/kg)	No. of survivors (day 60)	Mean survival time[a]	Median survival time[a]	% ILS[b]	*L*/*F*[b]
Control	0	0/12	9.08 ± 0.19	9.00 ± 0.21		
f-M	4	4/12	38.67 ± 3.54	36.00 ± 6.06	300	
Plm60	4	8/12	47.00 ± 2.88	n.a.	n.a.	n.a.
Plm80	4	4/12	39.17 ± 4.1	38.00 ± 11.26	322	1.06
Plm100	4	2/12	30.08 ± 3.59	23.00 ± 2.89	156	0.64

BDF1 mouse was inoculated with 5×10^5 cells i.p. on day 0 and treated on day1.
[a] To calculate mean and median survival times, survivors after 60 days were assigned survival time of 60 days.
[b] Values for ILS (increased life span) and liposomal/free (*L*/*F*) were calculated using median survival data. n.a., not applicable.

Table 5
Antitumor efficacy of MIT formulations against L1210 leukemia cell line in BDF1mice

Treatment group	Dose (mg/kg)	No. of survivors (day 60)	Mean survival time[a]	Median survival time[a]	% ILS[b]	*L*/*F*[b]
Control	0	0/6	11.83 ± 0.48	11.00		
f-M	2	0/8	12.13 ± 0.61	11.00	0	
f-M	4	0/8	13.25 ± 0.53	13.00 ± 0.46	18.2	
f-M	6	0/8	14.50 ± 0.71	14.00 ± 0.91	27.3	
Plm60	2	0/8	19.13 ± 1.57	18.00 ± 1.41	63.6	1.64
Plm60	4	3/8	36.50 ± 6.51	22.00 ± 5.66	100	1.69
Plm60	6	7/8	57.38 ± 2.46	n.a.	n.a.	n.a.
Plm60	8	8/8	n.a.	n.a.	n.a.	

Mice were inoculated with 5×10^4 cells i.v. on day 0 and treated on day 1.
[a] To calculate mean and median survival times, survivors after 60 days were assigned survival time of 60 days.
[b] Values for ILS (increased life span) and liposomal/free (*L*/*F*) were calculated using median survival data. n.a., not applicable.

that in all animals (control or treated), the tumor growth was governed by exponential equation ($V_t = V_0 e^{kt}$, wherein, *V* is tumor volume, *t* is time and *k* is growth constant.). Both plm60 and f-M could effectively inhibit the tumor growth, but at the same dose plm60 was more therapeutically active than f-M ($p < 0.01$) (Fig. 4). For example, the tumor doubling time in animals treated with 6 mg/kg plm60 was 4.9 days, about 1.6-folds higher than that of f-M group (Table 6).

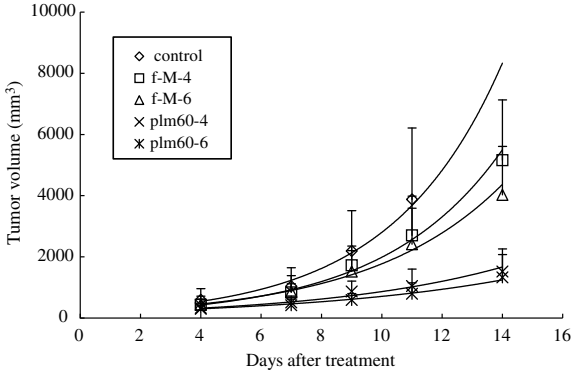

Fig. 4. The antineoplastic effect of plm60 and f-M in Rm-1 tumor model. When the tumor volume reached to ~0.2 cm^3, MIT formulations were injected into BDF1 mice via tail vein at 4 or 6 mg/kg ($n = 11$). To reveal the exponential growth of tumor, the tumor volume was plotted as a function of time and the exponential trend lines were also added.

4. Discussion

Most of chemotherapeutic agents are administrated to humans via intravenous injection. Due to their poor selectivity for malignant cells and non-specific distribution, these agents usually induce severe toxicity after intravenous administration. Liposome encapsulation has been proved to be an effective means to improving the therapeutic indexes of antineoplastic agents, which might be attributed to enhanced permeability and retention effects [8]. It should be noted, though, that only when liposomes could effec-

Table 6
The exponential growth of RM-1 tumor in BDF1 mice

Treatment group	Dose level (mg/kg)	r^2	p	V_0	k	Doubling time
Control	0	0.988	0.001	198	0.2608	2.66
f-M	4	0.992	0.000	156	0.2547	2.72
f-M	6	0.993	0.000	186	0.2256	3.07
Plm60	4	0.973	0.002	167	0.1645	4.21
Plm60	6	0.981	0.001	172	0.1416	4.90

RM-1 was inoculated into BDF1 with 5×10^5 cells/mouse. Fourteen days post inoculation, plm60 and f-M were administrated to BDF1 mice via tail vein at a dose of 4 or 6 mg/kg (11 mice/group). The mean tumor volume values were used to calculate the kinetic parameters ($V = V_0 \times e^{kt}$). The doubling time was calculated with LN(2)/k.

tively retain entrapped drugs in circulation and release drug at an optimum rate after accumulation into local tumors, could the therapeutic index be improved.

Accordingly, the manipulation of drug loading, retention and release characteristics is very important in the development of liposomal drugs. It is well known that weakly basic drugs could be loaded into liposomes in response to transmembrane pH gradient, in which method, after accumulation within vesicles, neutral drug molecules become protonated in acidic intraliposomal medium and are precipitated by anions such as sulfate or citrate [25–26]. The anions play an important role in the drug retention inside vesicles and the release from vesicles because they could form specific aggregation status with basic bioamines such as anthracyclines [27].

To date, three liposomal anthracyclines have been approved by regulatory authorities for the treatment of malignant tumors which include Doxil/Caelyx, Daunoxome and Myocet. Although there are no reports about the physical status of daunorubicin/citrate inside liposomes (Daunoxome), the aggregation forms of doxorubicin sulfate (Doxil/Caelyx) and doxorubicin citrate (Myocet) have been resolved using cryoelectronic technology [28–30]. Inside vesicles, doxorubicin could self-stack into fibers through hydrophobic interactions of anthracyclines and then interweave into bundles, which are bridged by anions such as sulfate and citrate. The release of doxorubicin from vesicles involves a series of steps including the dissipation of pH gradient, the deprotonation of doxorubicin, the dissolution of doxorubicin precipitate and the transmembrane movement of neutral doxorubicin molecules. Obviously, the aggregation status of doxorubicin inside vesicles strongly affects the drug-release kinetics. Despite that MIT is also a synthetic anthracenedione, it is different from doxorubicin because it has two physiologically dissociated groups (–NH–, pK_a = 8.13 [10]). Therefore, it is easy to understand that MIT would exhibit more complicated aggregation status with sulfate inside vesicles because not only one sulfate could interact with two different MIT, but also one MIT could combine with different sulfates, which is apparently compared to the case of doxorubicin.

Although the physical status of MIT/sulfate inside vesicles has not been resolved, the authors still believe that the complicated interactions of MIT with sulfate would preclude the dissociation of MIT from aggregates, thus affecting the release kinetics of MIT. The possession of multiple dissociated groups may affect not only the aggregation status of MIT/sulfate, but also the deprotonation and subsequent transmembrane transport of MIT.

Under the assumption that all the MITs inside vesicles become soluble, which might occur at the late stage of release studies and the transport of MIT across bilayers is governed by Fick's law, one could obtain

$$d[D]_i^{tot}/dt = -pA_m([D]_i - [D]_o)/V_i \quad (1)$$

wherein, $[D]_i^{tot}$ is the total concentration of MIT inside vesicles, p is permeability parameter, A_m is membrane area, and $[D]_i$, $[D]_o$ are the neutral form of MIT inside or outside vesicles.

Let k_1, k_1', k_2 and k_2' refer to the dissociation constants of MIT and $[H^+]_i$ is the interior proton concentration, $[D]_i$ could be expressed as

$$[D]_i = [D]_i^{tot}/(1 + [H^+]_i/k_1 + [H^+]_i^2/k_1k_1' + [H^+]_i^3/k_1k_1'k_2 + [H^+]_i^4/k_1k_1'k_2k_2') \quad (2)$$

We assume that $[H^+]_i \approx k_1$ and $k_1' >> k2$ and k_2'. This is reasonable for MIT, for which k_1 and $k_1' = 10^{-5.99}$ and k_2 and $k_2' = 10^{-8.13}$ [10]. Moreover, the intraliposomal pH might be slightly acidic [31]. Then we could obtain

$$[D]_i = [D]_i^{tot}(k_2k_2'/[H^+]_i^2) \quad (3)$$

Taking into account the fact that $[D]_i >> [D]_o$, and substituting (3) into (1), we could then obtain

$$d[D]_i^{tot}/dt = -[D]_i^{tot}pA_mk_2k_2'/([H^+]_i^2V_i) \quad (4)$$

Therefore, the release constant $K = pA_mk_2k_2'/([H^+]_i^2V_i)$.

Based on final equation, one should understand that even if the aggregation status is not considered, MIT is also hard to be released from vesicles compared to doxorubicin, because $k_2k_2'/[H^+]_i^2$ ($k_2, k_2' = 10^{-8.13}$) is much smaller than $k/[H^+]_i$ ($k = 10^{-8.15}$ [32]), which has been proved by in-vitro release studies. Here, $pA_mk/([H^+]_iVi)$ is the release constant of doxorubicin, which could be achieved using the similar formula deduction steps.

In this study, the small-sized vesicles were employed to accelerate the release rate of MIT from vesicles. The size reduction has at least two advantages. First, provided that MIT/lipid mass ratio is constant, small-sized formulations will contain more particles and each particle contains a small-sized MIT/sulfate precipitate. Quick calculation has revealed that the amount of vesicles is inversely proportional to the square of vesicle diameter. Accordingly, the precipitate inside small-sized formulations has a larger specific area than that inside large-sized formulations, which might facilitate the precipitate dissolution and subsequent drug release in accordance with the Ostwald–Freundlich equation

$$Ln(S/S_o) = 2M\gamma/\rho RT(1/r - 1/r_o)$$

where r is precipitate particle radius, ρ is density, γ is interfacial tension, T is temperature, M is molecular weight, R is gas constant, and S and S_o are the solubility of precipitate particles with radii r and r_o, respectively.

The second advantage lies in the fact that the reduction of size would increase the release constant K since K is inversely proportional to V_i. Because the release kinetics was governed by exponential equation,

$$[D]_{i\,(t)}^{tot} = [D]_{i\,(0)}^{tot}EXP(-Kt) \quad (5)$$

wherein, $[D]_{i\,(t)}^{tot}$ is the total concentration of MIT inside vesicles at time t, and $[D]_{i\,(0)}^{tot}$ is the total concentration of MIT inside vesicles at time 0.

The slight increase in K will lead to marked increase in drug release from vesicles. Perhaps, it is just because of these two effects, the release rate of MIT from small vesicles is significantly increased.

Besides these two effects, there are still other effects, which might affect drug release and need careful discussion. As shown in Table 1, small-sized vesicles are more negatively charged than large-sized vesicles, revealing that more peg-lipids redistributed in the outer layer during the preparation procedure. The higher peg-lipid content on the outer monolayer of SUVs might lead to packing defects in the bilayer and more rapid drug release. To test the effect of asymmetric distribution of peg-lipid on drug-release kinetics, we used an extreme example.

A formulation named pi-plm60 was prepared using "post insertion" technology [33]. It has the same components as plm60, but contained only half the amount of peg-lipids. Moreover, all the peg-lipids were grafted into the outer monolayer of the vesicles. The preparation of pi-plm60 was as follows. Briefly, we first prepared "non-stealth" version of plm60 (lm60), which was done in accordance with the procedure for the preparation of plm60, but contained no peg-lipids in the formulation. And then, 50% amount of peg-lipids was incubated with lm60 at 60 °C for 1 h, resulting in the pegylation of the outer monolayer of lm60. Under the above conditions, the insertion efficiency of peg-lipids into outer layer of lm 60 was ~100%, and we have proved this via Sepharose 4B separation and HPLC analysis.

In-vitro release studies revealed that the overall release kinetics of plm60 and pi-plm60 exhibited no difference ($p > 0.05$, two-way ANOVA). Therefore, the effects of asymmetric distribution of peg-lipids in small-sized formulations might be negligible.

As for lipid bilayer compositions, they were almost similar in different vesicles even after sample preparation based on HPLC analysis. The homogenization with Microfluidizer did not increase the amount of lyso PC compared to extrusion. Since only ~0.9% HPLC was hydrolyzed during the preparation, it should not affect the drug-release rate.

Because the small-sized pegylated MIT formulation has the faster drug-release rate, more MIT will be released from vesicle and become bioavailable after the accumulation within tumor, thus leading to enhanced antitumor efficacy in all tumor models.

Fortunately, the fast-release formulation (plm60) is only a little more toxic than the other two formulations (plm80 and plm100) and its skin toxicity is less severe. In addition, plm60 is at least 2–3 times less toxic than f-M in KM mice. The improved therapeutic index of plm60 should be attributed to changed biodistribution and different drug-release rate of plm60 in tumor and normal tissues. As proved in previous studies, tumor microenvironment might facilitate drug release relative to normal tissue [34]. Therefore, the acute toxicity of plm60 is similar to plm80 and plm100, but it is more efficacious. If the HSPC in plm60 is replaced by DPPC or DMPC, the drug-release rate will be further increased, leading to more toxic formulations. For example, when plm60-DMPC (a formulation similar to plm60, but DMPC was employed instead of HSPC) was injected into balb/c at a dose of 6 mg/kg, 100% mice died in ~3days, and at this dose level f-M and plm60 could be well-tolerated by balb/c mice. The example clearly proved that plm60 might be an optimum formulation (unpublished data). Size reduction could also enhance the antitumor efficacy of liposomal MIT formulations when MIT was loaded with transitional metal gradient method (unpublished data).

In all, MIT possesses multiple physiologically dissociated groups, and could form complicated aggregation status with polyanions inside liposomes, thus precluding the dissociation of MIT from MIT/sulfate precipitates. Moreover, even in the case that intraliposomal precipitate becomes soluble, the release constant of MIT is still low relative to other anthracyclines such as doxorubicin due to the presence of multiple dissociated groups in MIT. The reduction of vesicle size could increase the specific area of MIT/sulfate precipitate inside vesicle and the release constant K, which is inversely proportional to vesicle volume ($K = pA_m k_2 k_{2'} / ([H^+]_i^2 V_i)$). Therefore, the employment of small-sized formulations could accelerate drug release and then enhance antitumor effects of MIT in RM-1, L1210 ascitic and liver metastasis models.

References

[1] O. Neuhaus, B.C. Kieseier, H.P. Hartung, Mitoxantrone in multiple sclerosis, Adv. Neurol. 98 (2006) 293–302.

[2] C.J. Dunn, K.L. Goa, Mitoxantrone: a review of its pharmacological properties and use in acute nonlymphoblastic leukaemia, Drugs Aging 9 (2) (1996) 122–147.

[3] L.R. Wiseman, C.M. Spencer, Mitoxantrone. A review of its pharmacology and clinical efficacy in the management of hormone-resistant advanced prostate cancer, Drugs Aging 10 (6) (1997) 473–485.

[4] R.S. Benjamin, Rationale for the use of mitoxantrone in the older patient: cardiac toxicity, Semin. Oncol. 22 (1 S11) (1995) 11–13.

[5] E.C. van Dalen, H.J. van der Pal, P.J. Bakker, H.N. Caron, L.C. Kremer, Cumulative incidence and risk factors of mitoxantrone-induced cardiotoxicity in children: a systematic review, Eur. J. Cancer 40 (5) (2004) 643–652.

[6] T.J. Murray, The cardiac effects of mitoxantrone: do the benefits in multiple sclerosis outweigh the risks?, Expert Opin Drug Saf. 5 (2) (2006) 265–274.

[7] N. Kroger, L. Damon, A.R. Zander, H. Wandt, G. Derigs, P. Ferrante, T. Demirer, G. Rosti, Secondary acute leukemia following mitoxantrone-based high-dose chemotherapy for primary breast cancer patients, Bone Marrow Transplant. 32 (12) (2003) 1153–1157.

[8] D.C. Drummond, O. Meyer, K. Hong, D.B. Kirpotin, D. Papahadjopoulos, Optimizing liposomes for delivery of chemotherapeutic agents to solid tumors, Pharmacol. Rev. 51 (4) (1999) 691–743.

[9] S. Ugwu, A. Zhang, M. Parmar, B. Miller, T. Sardone, V. Peikov, I. Ahmad, Preparation, characterization, and stability of liposome-based formulations of mitoxantrone, Drug Dev. Ind. Pharm. 31 (2) (2005) 223–229.

[10] A. Ahmad, Y.F. Wang, I. Ahmad, Separation of liposome-entrapped mitoxantrone from nonliposomal mitoxantrone in plasma: pharmacokinetics in mice, Methods Enzymol. 391 (2005) 176–185.

[11] P.C. Gokhale, J. Pei, C. Zhang, I. Ahmad, A. Rahman, U. Kasid, Improved safety, pharmacokinetics and therapeutic efficacy profiles of a novel liposomal formulation of mitoxantrone, Anticancer Res. 21 (5) (2001) 3313–3321.

[12] R. Reszka, P. Beck, I. Fichtner, M. Hentschel, J. Richter, J. Kreuter, Body distribution of free, liposomal and nanoparticle-associated mitoxantrone in B16-melanoma-bearing mice, J. Pharmacol. Exp. Ther. 280 (1) (1997) 232–237.

[13] K.M. Rentsch, D.H. Horber, R.A. Schwendener, H. Wunderli-Allenspach, E. Hanseler, Comparative pharmacokinetic and cytotoxic analysis of three different formulations of mitoxantrone in mice, Br. J. Cancer 75 (7) (1997) 986–992.

[14] R.A. Schwendener, H.H. Fiebig, M.R. Berger, D.P. Berger, Evaluation of incorporation characteristics of mitoxantrone into unilamellar liposomes and analysis of their pharmacokinetic properties, acute toxicity, and antitumor efficacy, Cancer Chemother. Pharmacol. 27 (6) (1991) 429–439.

[15] B.C. Pestalozzi, A. Vass, H. Adam, D.H. Horber, R.A. Schwendener, C. Sauter, Phase II study of liposome-complexed mitoxantrone in patients with advanced breast cancer, Eur. J. Cancer 31 (6) (1995) 1024.

[16] B. Pestalozzi, R. Schwendener, C. Sauter, Phase I/II study of liposome-complexed mitoxantrone in patients with advanced breast cancer, Ann. Oncol. 3 (6) (1992) 445–449.

[17] H.J. Lim, M.J. Parr, D. Masin, N.L. McIntosh, T.D. Madden, G. Zhang, S. Johnstone, M.B. Bally, Kupffer cells do not play a role in governing the efficacy of liposomal mitoxantrone used to treat a tumor model designed to assess drug delivery to liver, Clin. Cancer Res. 6 (11) (2000) 4449–4460.

[18] H.J. Lim, D. Masin, N.L. McIntosh, T.D. Madden, M.B. Bally, Role of drug release and liposome-mediated drug delivery in governing the therapeutic activity of liposomal mitoxantrone used to treat human A431 and LS180 solid tumors, J. Pharmacol. Exp. Ther. 292 (1) (2000) 337–345.

[19] G. Adlakha-Hutcheon, M.B. Bally, C.R. Shew, T.D. Madden, Controlled destabilization of a liposomal drug delivery system enhances mitoxantrone antitumor activity, Nat. Biotechnol. 17 (8) (1999) 775–779.

[20] H.J. Lim, D. Masin, T.D. Madden, M.B. Bally, Influence of drug release characteristics on the therapeutic activity of liposomal mitoxantrone, J. Pharmacol. Exp. Ther. 281 (1) (1997) 566–753.

[21] C.W. Chang, L. Barber, C. Ouyang, D. Masin, M.B. Bally, T.D. Madden, Plasma clearance, biodistribution and therapeutic properties of mitoxantrone encapsulated in conventional and sterically stabilized liposomes after intravenous administration in BDF1 mice, Br. J. Cancer 75 (2) (1997) 169–177.

[22] J.X. Cui, C.L. Li, W.M. Guo, Y.H. Li, C.X. Wang, L. Zhang, L. Zhang, Y.L. Hao, Y.L. Wang, Direct comparison of two pegylated liposomal doxorubicin formulations: is AUC predictive for toxicity and efficacy?, J Control. Release 118 (2) (2007) 204–215.

[23] M.C. Woodle, D.D. Lasic, Sterically stabilized liposomes, Biochim. Biophys. Acta 1113 (2) (1992) 171–199.

[24] A. Gabizon, H. Shmeeda, Y. Barenholz, Pharmacokinetics of pegylated liposomal doxorubicin: review of animal and human studies, Clin. Pharmacokinet. 42 (5) (2003) 419–436.

[25] T.D. Madden, P.R. Harrigan, L.C. Tai, M.B. Bally, L.D. Mayer, T.E. Redelmeier, H.C. Loughrey, C.P. Tilcock, L.W. Reinish, P.R. Cullis, The accumulation of drugs within large unilamellar vesicles exhibiting a proton gradient: a survey, Chem. Phys. Lipids 53 (1) (1990) 37–46.

[26] G. Haran, R. Cohen, L.K. Bar, Y. Barenholz, Transmembrane ammonium sulfate gradients in liposomes produce efficient and stable entrapment of amphipathic weak bases, Biochim. Biophys. Acta 1151 (2) (1993) 201–215.

[27] D.C. Drummond, M.E. Hayes, C.O. Noble, J.W. Park, D.B. Kirpotin, Z. Guo, Intraliposomal trapping agents for improving in vivo liposomal drug formulation stability, in: G. Gregoriadis (Ed.), Liposome Technology, Informa Healthcare USA, Inc., New York, 2007, pp. 149–168.

[28] D.D. Lasic, P.M. Frederik, M.C. Stuart, Y. Barenholz, T.J. McIntosh, Gelation of liposome interior. A novel method for drug encapsulation, FEBS Lett. 312 (2–3) (1992) 255–258.

[29] X. Li, D.J. Hirsh, D. Cabral-Lilly, A. Zirkel, S.M. Gruner, A.S. Janoff, W.R. Perkins, Doxorubicin physical state in solution and inside liposomes loaded via a pH gradient, Biochim. Biophys. Acta 1415 (1) (1998) 23–40.
[30] D.D. Lasic, B. Ceh, M.C. Stuart, L. Guo, P.M. Frederik, Y. Barenholz, Transmembrane gradient driven phase transitions within vesicles: lessons for drug delivery, Biochim. Biophys. Acta 1239 (2) (1995) 145–156.
[31] Y. Barenholz, Amphipathic weak base loading into preformed liposomes having a transmembrane ammonium ion gradient: from the bench to approved doxil, in: G. Gregoriadis (Ed.), Liposome Technology, Informa Healthcare USA, Inc., New York, 2007, pp. 1–26.
[32] S.A. Abraham, D.N. Waterhouse, L.D. Mayer, P.R. Cullis, T.D. Madden, M.B. Bally, The liposomal formulation of doxorubicin, in: N. Duzgunes (Ed.), Liposomes, Elsevier Inc., 2005, pp. 71–97.
[33] D.L. Iden, T.M. Allen, In vitro and in vivo comparison of immunoliposomes made by conventional coupling techniques with those made by a new post-insertion approach, Biochim. Biophys. Acta 1513 (2) (2001) 207–216.
[34] A.A. Gabizon, Liposome circulation time and tumor targeting: implications for cancer chemotherapy, Adv. Drug Deliv. Rev. 16 (2–3) (1995) 285–294.